Desalination and Water Treatment
www.deswater.com

doi: 10.5004/dwt.2020.25245

188 (2020) 232–238
June

Adsorption of methylene blue from effluent using golden mussel (*Limnoperna fortunei*) shell as a low-cost material

Daniel Mantovani[a,b,*], Heloise Beatriz Quesada[a], Rodrigo de Souza Antônio[a], Luis Fernando Cusioli[a], Letícia Nishi[a], Alexandre Diório[a], Paulo Fernando Soares[c], Rosângela Bergamasco[a], Marcelo Fernandes Vieira[a]

[a]*State University of Maringa, Department of Chemical Engineering, Maringa 87020-900, Parana, Brazil, Tel. +55-44-3011-4782; emails: daniel26mantovani@gmail.com (D. Mantovani), heloisequesada@gmail.com (H.B. Quesada), z.rodrigo.antonio@gmail.com (R. de Souza Antônio), luiscusioli@gmail.com (L.F. Cusioli), leticianishi@hotmail.com (L. Nishi), diorio.alexandre@gmail.com (A. Diório), rbergamasco@uem.br (R. Bergamasco), mfvieira2@uem.br (M.F. Vieira)*
[b]*Department of Chemical Engineering, State University of Maringá, 5790 Colombo avenue, Building D-90, CEP 87020-900 Maringá, Brazil*
[c]*Graduate Program in Urban Engineering, State University of Maringá, Zip code: 87020-900 Maringá, Brazil, Tel: +55-44-3011-4782; email: pfsoares@uem.br (P.F. Soares)*

Received 2 August 2019; Accepted 24 November 2019

ABSTRACT

The golden mussel is a species from China, which has spread to Asia and America, causing various economic impacts, as well as an ecological imbalance. Globally, the application of the invasive species has been investigated to mitigate the problems caused, and the present work evaluates the use of the golden mussel shells in the removal of methylene blue from contaminated waters. The material was characterized by the analysis of scanning electron microscopy, X-ray fluorescence, Fourier transform infrared spectroscopy and zeta potential, indicating favorable characteristics for the adsorption of pollutants. As for the adsorption studies, the adjustment of the pseudo-first-order model was verified, resulting in adsorption capacity of 26.4 mg g^{-1} at the equilibrium time of 300 min and 0.03 g of adsorbent. Henry's model was applied at 25°C, 35°C, and 45°C indicating the favorable effect of temperature increase. Thus, it is observed the potential of using this material as adsorbent of water contaminants.

Keywords: Golden mussel; *Limnoperna fortunei*; Adsorption; Methylene blue; Effluent

1. Introduction

Water pollution occurs when chemicals such as fertilizers, dyes, pesticides, and petroleum derivatives reach water bodies. These substances are found in effluents, due to inadequate treatment, and are produced in anthropic activities such as agriculture and industrial and domestic activities [1].

The industrial activities are the greatest consumer of water and, consequently, produces a considerable amount of effluent that needs proper treatment before being released into the environment. The textile, pulp and paper, and polymer industries use several types of dyes in their products [2], the discharge of these effluents does not only affect the environment aesthetics, but also the sunlight infiltration into the water's surface, which leads to a reduction of the photosynthetic activity. In this way, this process causes several impacts to aquatic organisms due to insufficient oxygen [3].

* Corresponding author.

Methylene blue (MB) is a cationic dye widely used in anthropic activities in textile industries. When ingested, MB produces a burning sensation and can cause nausea, vomiting, diarrhea, and gastritis. In the environment, MB has several detrimental effects when present in water bodies [4,5].

In this way, it is possible to emphasize the importance of performing the treatment of industrial effluents to remove MB and other dyes. The treatment aims to prevent that the effluent pollutants reach the water bodies and, therefore, prevent environmental deterioration and human health damages. The removal methodologies that aimed the treatment of effluents contaminated by MB are coagulation/flocculation, photocatalysis, photo-Fenton, electro-Fenton and adsorption [6–9].

Adsorption is considered a promising treatment process due to its low cost, simple design and easy operation. However, for the effluents' treatment, the adsorbent material must present characteristics of high thermal and physical resistance, as well as affinity with the substance to be adsorbed, thus choosing the adsorbent dependent on a series of factors. Therefore, the material must have high availability of adsorption sites and a large amount of carbon and oxygen [10]. The diversity of raw materials that can be used in the development of adsorbents makes it interesting to exploit residual biomass, and this concept has led to the popularity of the term 'low-cost adsorbents' [11,12].

In this study, we choose to produce a low-cost adsorbent from the golden mussel (*Limnoperna fortunei*) shell. The golden mussel is a widespread invasive freshwater mussel from China and invasively spreading to many Asian and South American countries by the discharge of ships ballast water containing high concentrations of mussel larvae. [13–15]. It easily invades water transfer works and attaches onto concrete walls and structures with extremely high density, resulting in biofouling, structure corrosion, pipe clogging, decrease in water transfer efficiency, water pollution, and other disadvantages, and has become a prevalent problem which is causing global concern [16]. This mussel has been causing many losses due to its incrustation in vessel hulls, tanks, and fishing nets. Several attempts to eliminate the golden mussel were frustrated, so the best proposal in the researcher's view is to find possible uses to this invading mollusk to productive activities [17,18].

Currently, shells of different species of mussels are being used to remove heavy metals and textile dyes from contaminated water [19–21]. However, it is not known of reports that use in natural biomass of the golden mussel's shell (*Limnoperna fortunei*) as adsorbent material of water pollutants. Therefore, the objective of this work was to evaluate the adsorption capacity of the MB dye from aqueous samples using the biomass of *Limnoperna fortunei* as a low-cost adsorbent.

2. Materials and methods

2.1. Preparation of the adsorbent from golden mussel's shell

The golden mussel's shell was obtained from Usina Hidrelétrica de Rosana, São Paulo, Brazil. The geographical coordinates of the hydroelectric plant are 22°36′07″S and 52°52′20″ W.

Firstly, the shells were manually washed with tap water for 30 min at room temperature. The washing process was repeated 6 times to remove water-soluble impurities. Then, the shells were dried in an incubator with air circulation (SXCR 42, Sterilifer©, Brazil) at 80°C for 24 h.

After that, the shells were ground using a domestic blender and sieved to different mesh sizes in a magnetic stirrer type (Bertel). For the experiments, the average particle size of 600 μm was chosen as the particle size at which most of the particles were retained.

2.2. Characterization of the adsorbent

The morphological characteristics of the surface of the golden mussel's shell adsorbent (GMA) were evaluated by scanning electron microscopy (SEM) with the aid of a Quanta FEI microscope, model 250, operating at 25 kV. For this analysis, the samples were covered with gold at a thickness of approximately 30 nm.

The zeta potential was measured using a sample with 0.05 g of adsorbent in 50 mL of water using a Delsa™ NanoC by Beckman Coulter (TM) equipment. The pH was measured using a pH meter (Orion™ Versa Star Benchtop Meter, Thermo Scientific™, USA). The pH was adjusted from 3 to 12, with HCl 0.1 M and/or NaOH 0.1 M.

To characterize the functional groups present in the golden mussel's shell, a Fourier transform infrared (FTIR) spectrometer (PerkinElmer Spectrum100, USA) was used. Tablets were prepared by mixing powder samples with KBr (Sigma-Aldrich) at the ratio of 1:100 (w/w). The spectral range varied from 4,000 to 400 cm^{-1}.

The X-ray fluorescence (FRX) analysis of the golden mussel's shell employed a spectrometer Bruker S8 model Tiger 4 kW. For this analysis, 1.0 g of the ground samples were mixed with 20 g of boric acid in an agate mortar and, after homogenization, 7.0 g of the mixture was compressed in a pellet prior to analysis.

2.3. Adsorption of MB

The MB adsorption using golden mussel's shell was conducted in a closed and batch system. The experiments were performed with 25 mL of MB solution samples prepared at a concentration of 50 mg L^{-1} in distilled water in Erlenmeyer flask with a stopper. The flasks were shaken on a shaker (QUIMIS® 0022MI, Brazil) at 150 rpm, at room temperature, for 24 h. The adsorption assays were performed with different adsorbent mass: 0.03, 0.05, 0.1, 0.2, and 0.4 g.

Samples were collected after 24 h and then filtered through a cellulose acetate filter (0.45 μm diameter pore) to remove the adsorbent. After filtering, the sample was then measured by a UV-Vis spectrophotometer (HACH DR 5000) at a wavelength of 665 nm. All assays were performed in duplicates.

The MB adsorption capacity (mg g^{-1}) was calculated using Eq. (1):

$$q_e = \frac{\left(C_0 - C_t\right)V}{m} \tag{1}$$

In Eq. (1), C_0 is the initial concentration of MB (mg L^{-1}), C_t is the equilibrium concentration in solution (mg L^{-1}) in time t, V is the solution volume (L), and m is sorbent mass (g).

The kinetic study was performed in batch with the adsorbent mass that resulted in the best q_e, in contact with 25 mL of 50 mg L^{-1} MB solution, maintained at a stirring speed of 150 rpm and controlled temperature of 25°C. The time intervals for withdrawing the aliquots from the analyzed samples were 1–720 min, the flasks were shaken with the aid of an orbital shaker table after the contact time, the final MB concentration readings were performed as described above, using a spectrophotometer at 665 nm, and the tests were performed in duplicates.

To explain the kinetic mechanism, the two best-known models were applied to the experimental data: the pseudo-first-order, proposed by Lagergren [22], and pseudo-second-order model, proposed by Ho and McKay [23], which are presented by Eqs. (2) and (3), respectively.

$$q_t = q_e\left[1 - e^{-k_1 t}\right] \tag{2}$$

where k_1 is the constant of the first-order adsorption rate (min^{-1}) and q_e and q_t are the adsorbed amounts per g of adsorbent at equilibrium and at time t, respectively (mg g^{-1}).

$$q_t = \frac{k_2 q_e^2 t}{1 + k_2 q_e t} \tag{3}$$

where k_2 is the constant of the pseudo-second-order adsorption rate (g mg^{-1} min^{-1}).

The equilibrium isotherms were obtained at temperatures of 25°C, 35°C, and 45°C. The tests were conducted with MB concentration from 5 to 200 mg L^{-1} that was varied in a solution volume of 25 ml. Samples were agitated in a shaking incubator (model TE-4200 TECNAL) at 150 rpm and the contact time was 720 min.

An application of Henry's constant was performed. The Isotherm of Henry is a linear adsorbent isotherm model in which the amount of surface adsorbate is proportional to the adsorbate concentration in the fluid at equilibrium conditions [24]. The equilibrium concentrations of adsorbate in the liquid and adsorbed phases are related to the linear expression as shown in Eq. (4):

$$q_e = K \times C_e \tag{4}$$

where q_e is the amount of the adsorbate at equilibrium (mg g^{-1}), K is Henry's adsorption constant (L g^{-1}), and C_e is the equilibrium concentration of the adsorbate on the adsorbent (mg L^{-1}).

The results were analyzed for correlation coefficient (R^2) and chi-square (χ^2) (Eq. (5)).

$$\chi^2 = \sum_{i=1}^{n} \frac{\left(x_i - m_i\right)^2}{m_i} \tag{5}$$

where x is the experimental value and m is the expected value for the mathematical model.

3. Results and discussion

3.1. Characterization of the adsorbent

Fig. 1 shows the SEM images of the golden mussel's shell at 5,000× magnification. The SEM of the sample showed that the morphology did not have regular shape and size and presented heterogeneity of pores. The samples

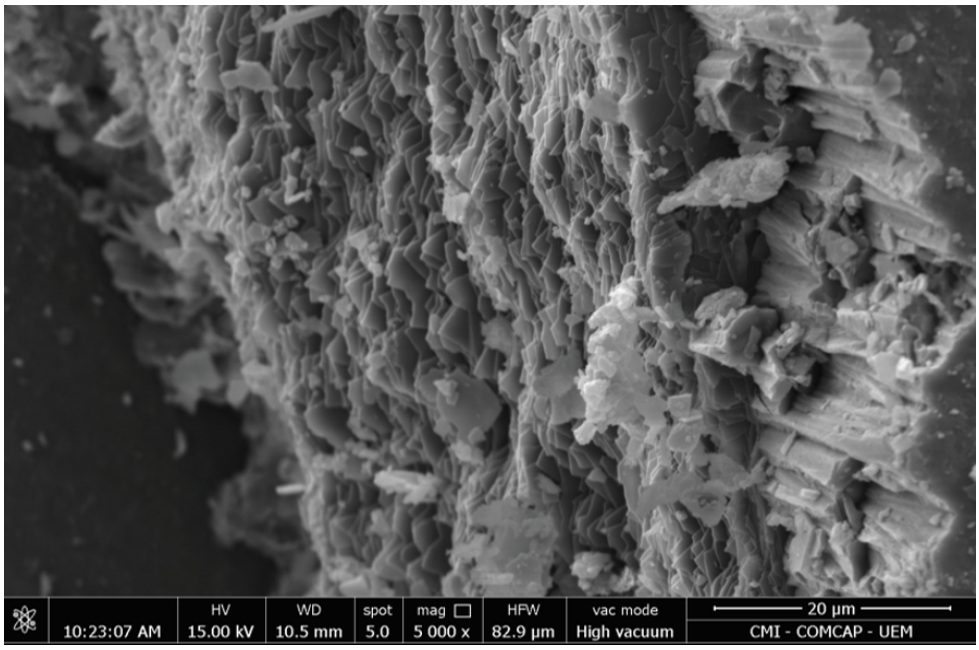

Fig. 1. Morphological structure of the golden mussel's shell.

presented an irregular surface with open pores, being favorable to the adsorption capacity of the adsorbent.

Fig. 2 shows the FTIR analysis where the functional groups present in the golden mussel's shell was determined before and after the MB adsorption.

It is seen that the IR spectrum of golden mussel's shell showed a characteristic Fourier transform IR band at 1,483 cm^{-1}, which was attributed to the C–O bond of the carbonate groups present in abundance in the shell [25]. The wideband at 3,279 cm^{-1} indicated the presence of hydrogen bonds (–OH) due to water molecules adsorbed in the golden mussel's shell surface. The peak present in the 2,923 cm^{-1} region indicated the presence of a C–H bond due to the protein composition of the adsorbent [26].

Vibrations observed in the range of 1,647, 1,448, and 850 cm^{-1} refer to carbonate CO bonds out of the plane and at 713 cm^{-1} of plane bending, as well as the vibrations detected at 1,780 and 1,082 cm^{-1} related to the CO bonds of carbonate ions [27,28]. Finally, the vibrations found in the wavelength of 536 cm^{-1} were attributed to the Ca–O binding, also present in the shell structure of the mussel [29].

Regarding the vibrations detected in the shell of the mussel adsorbed with MB, it was possible to affirm that there was no significant change when compared to the bark of the non-adsorbed mussel, however, it is possible to detect fewer changes in the wavelength range of 1,729 to 1,585 cm^{-1} and a displacement of the vibration band between the range of 890 to 750 cm^{-1} which are vibrations relating to the C–O bond of carbonates.

From the FRX analysis, it was possible to state that there was a significant amount of inorganic compounds present in the shell structure of the mussel. This was confirmed with the FRX analysis which detected a large proportion of oxides and other inorganic materials in the material. The results indicated calcium and silica oxides as being the majority of substances in the mussel shell's structure, respectively, 68.6% and 12.5%. Other compounds were found in trace concentrations or were not relevant to this research.

The zeta potential analysis of the golden mussel's shell is shown in Fig. 3. The values referring to the surface charge coming from the Zeta potential for the crushed golden mussel were: 28.3, 12.2, 8.8, –0.9, –2.89, –6.97, –14.57, –17.57, –22.8 e –26.43 (mV) in pH ranging from 3 to 12, respectively. This characteristic is mainly due to the presence of carbonate groups present in the shells.

Since MB is a cationic dye, an electronegative adsorbent would be more effective to remove MB from aqueous solution, in this way the pH 6.03, that is the natural pH of MB solution was used in the adsorption experiments. In this pH, the golden mussel's shell is electronegatively charged and it is not necessary to control the pH of the adsorption process.

3.2. Adsorption experiments

To evaluate the effect of adsorbent mass, the experiments were carried out while varying the mass from 0.03 to 0.4 g of golden mussel's shell (Fig. 4). For this, the MB concentration solution at 50 mg L^{-1}, temperature of 25°C, pH 6.03, and stirring speed of 150 rpm were kept constant.

One can see that the amount of MB adsorbed was found to be rapid from 0.03 to 0.05 g of golden mussel's shell. Further increase of adsorbent mass resulted in less increase in adsorption, and hence, 0.03 g was considered the optimum dose of the adsorbent.

Fig. 5 displays the results from the adsorption kinetics experiments and the fits of the pseudo-first-order and pseudo-second-order models to the data obtained for MB adsorption. The agitation time varied from 1 to 3,000 min and 50 mg L^{-1} of the MB solution was used at pH 6.03, as previously established. The kinetic model parameters fitted to the experimental data are shown in Table 1.

It can be seen in Fig. 5 that the MB adsorption did not change after 300 min, thus achieving the equilibrium state with concentration constant at, approximately, 26.4 mg g^{-1}. Lonappan et al. [30] studied the MB adsorption using activated carbon synthesized from three different residues (Pinus

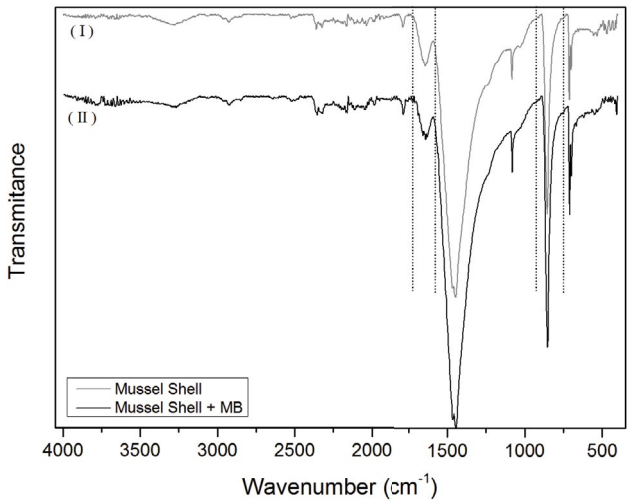

Fig. 2. FTIR spectra of golden mussel's shell before (I) and after (II) the MB adsorption.

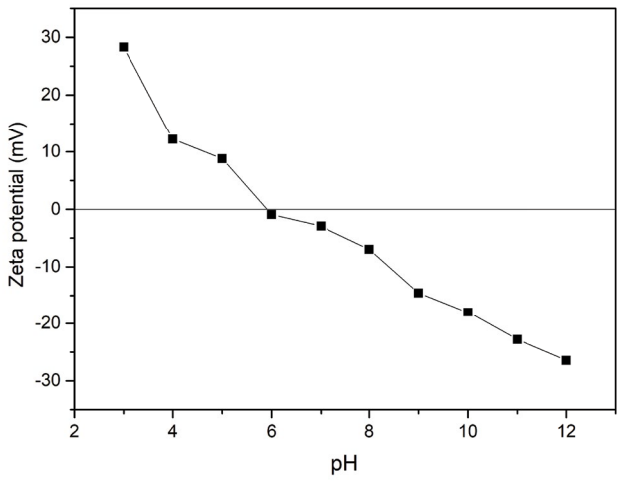

Fig. 3. Zeta potential of golden mussel's shell for different pH values.

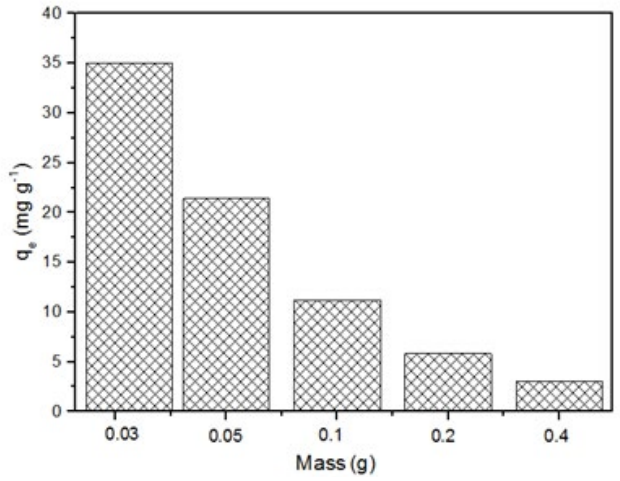

Fig. 4. MB adsorption capacity as a function of golden mussel's shell adsorbent mass.

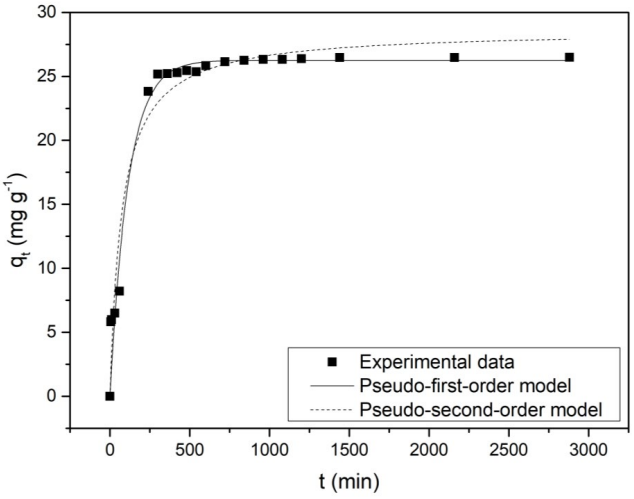

Fig. 5. Experimental kinetic data and fitting of MB adsorption capacity by golden mussel's shell.

trunk, pig manure, and paper). The authors determined the adsorption capacity of MB in these carbons as 1.32, 4.87, and 5.01 mg g^{-1}, respectively, showing that the golden mussel's shell had a greater capacity when in comparison. It is worth to note that, in this work, the golden mussel's shells had no modification prior to the adsorption process.

Regarding the kinetic models' parameters shown in Table 1, both pseudo-first and pseudo-second-order models presented R^2 values greater than 0.950. Nonetheless, analyzing the calculated adsorption capacity and the statistical χ^2, it was found that the pseudo-first-order model better fitted the experimental data. This model indicates that the MB adsorption over time is directly proportional to the difference in the saturation concentration of MB and the available activated sites in the mussel's shell surface [23,31].

It is important to state that the pseudo-first-order model equation is valid only when: the adsorption is in the Henry

Table 1
Kinetic and statistic parameters for the MB adsorption by golden mussel's shell

Models	Parameters	Values
Pseudo-first-order	$q_{e,calc}$ (mg g^{-1})	26.261
	k_1 (min^{-1})	0.009
	R^2	0.970
	χ^2	2.503
Pseudo-second-order	$q_{e,calc}$ (mg g^{-1})	28.620
	k_2 (g mg^{-1} min^{-1})	4.721
	R^2	0.958
	χ^2	3.553

range of concentrations or when the biosorbent mass is high [31–33]. The results found here are in agreement with the ones reported by Bedin et al. [34] for the adsorption of MB with KOH-activated carbon prepared from sucrose spherical carbon.

The isotherms were illustrated by plotting the amount of MB adsorbed on the golden mussel's shell at equilibrium (q_e) vs. the equilibrium concentration of MB in solution (C_e). The equilibrium uptake data obtained at 25°C, 35°C, and 45°C is shown in Fig. 6. The results obtained by fitting the Henry's Isotherms model to the experimental data are given in Table 2, which lists the parameters of this model.

From Fig. 6, it was possible to verify the applicability of Henry's model for all temperatures ($R^2 > 0.954$), corroborating with the pseudo-first-order model suggestion. Also, that the increase in temperature favors the adsorption capacity of the material, suggesting that the adsorption process of the MB in the shell of the golden mussel is endothermic. This finding can be confirmed by analyzing Table 2 and observing that the value of the Henry's constant increases with the increase in temperature from 25°C to 45°C.

The available literature for the adsorption using the Henry model is rare but a few are reported as a linear model. Nam et al. [35] reported that the adsorption of hydrophilic contaminants ($\log K_{ow} < 2.5$) agree with the Henry (linear) model using coconut shell as biosorbent, but the adsorption of hydrophobic contaminants agree with the Freundlich model. According to Mellish et al. [36], the MB is a hydrophilic contaminant ($K_{ow} = 0.75$), which agrees with the findings of this work.

4. Conclusion

The presence of contaminants as the MB in effluents discharged in the environment is of major concern due to environmental and health problems. In this sense, this paper aimed to produce a low-cost adsorbent from golden mussel (*Limnoperna fortunei*) shell, an invasive specimen, to remove the MB from aqueous solutions. From the results collected from FTIR, energy-dispersive X-ray spectroscopy and FRX, it was possible no affirm that the golden mussel's shell composition was predominant of oxides, characteristic of this living being. Regarding the adsorption of MB process, it was possible to remove great quantities of MB with a low mass of biosorbent, that is, in Henry's region of concentrations,

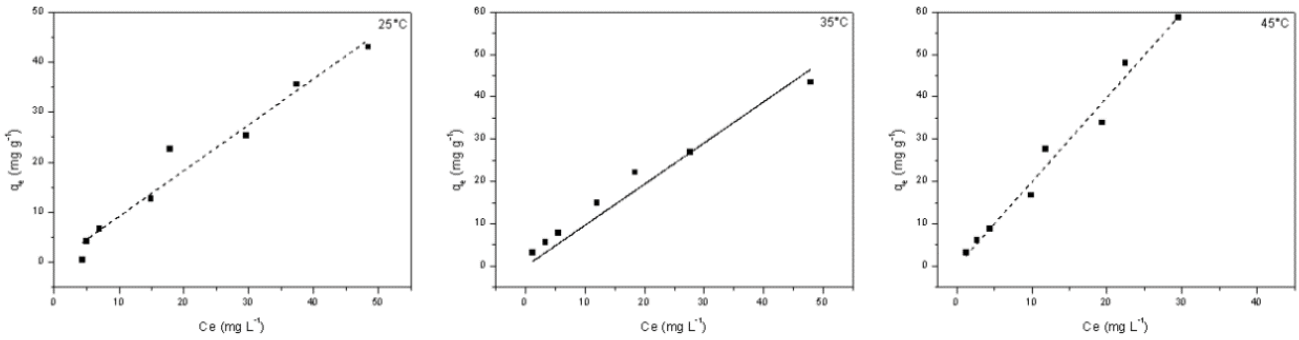

Fig. 6. Adsorption equilibrium of MB by golden mussel's shell.

Table 2
Henry's isotherm model applied to MB adsorption experiments

Temperature (°C)	Henry's constant	Values
25	K	0.917
	R^2	0.963
	χ^2	8.641
35	K	0.969
	R^2	0.954
	χ^2	9.316
45	K	1.993
	R^2	0.980
	χ^2	8.312

with Henry's model constant equal to 0.917 and increasing with the process temperature being, therefore, favorable for the process. For the kinetic experiments, the pseudo-first-order was the best-fitted model to explain the experimental results with an equilibrium time of 300 min. The golden mussel's shell MB adsorption capacity found was 26.4 mg g^{-1}. In conclusion, since the biosorbent was produced from an invasive specimen, it was possible to produce a low-cost and high-capacity biosorbent for the removal of contaminant MB from aqueous solution.

Acknowledgment

The authors are thankful to CAPES (Coordination for the Improvement of Higher Education Personnel) process number: 88882.315821/2019-01 and Araucária Foundation by financial support.

References

[1] G. Crini, P.M. Badot, Application of chitosan, a natural aminopolysaccharide, for dye removal from aqueous solutions by adsorption processes using batch studies: a review of recent literature, Prog. Polym. Sci., 33 (2008) 399–447.
[2] G. Crini, Non-conventional low-cost adsorbents for dye removal: a review, Bioresour. Technol., 97 (2006) 1061–1085.
[3] C. Namasivayam, R. Radhika, S. Suba, Uptake of dyes by a promising locally available agricultural solid waste: coir pith, Waste Manage., 21 (2001) 381–387.
[4] E.A. El-Sharkawy, A.Y. Soliman, K.M. Al-Amer, Comparative study for the removal of methylene blue via adsorption and photocatalytic degradation, J. Colloid Interface Sci., 310 (2007) 498–508.
[5] Y.L. Ma, Z.R. Xu, T. Guo, P. You, Adsorption of methylene blue on Cu(II)-exchanged montmorillonite, J. Colloid Interface Sci., 280 (2004) 283–288.
[6] D. Balarak, J. Jaafari, G. Hassani, Y. Mahdavi, I. Tyagi, S. Agarwal, V.K. Gupta, The use of low-cost adsorbent (Canola residues) for the adsorption of methylene blue from aqueous solution: isotherm, kinetic and thermodynamic studies, Colloids Interface Sci. Commun., 7 (2015) 16–19.
[7] K. Tahir, A. Ahmad, B. Li, S. Nazir, A.U. Khan, T. Nasir, Z.U.H. Khan, R. Naz, M. Raza, Visible light photo catalytic inactivation of bacteria and photo degradation of methylene blue with Ag/TiO_2 nanocomposite prepared by a novel method, J. Photochem. Photobiol., B, 162 (2016) 189–198.
[8] X. Yang, W. Chen, J. Huang, Y. Zhou, Y. Zhu, C. Li, Rapid degradation of methylene blue in a novel heterogeneous Fe_3O_4@rGO@TiO_2-catalyzed photo-Fenton system, Sci. Rep., 5 (2015) 1–10.
[9] D.A.G. Sumalinog, S.C. Capareda, M.D.G. de Luna, Evaluation of the effectiveness and mechanisms of acetaminophen and methylene blue dye adsorption on activated biochar derived from municipal solid wastes, J. Environ. Manage., 210 (2018) 255–262.
[10] I. Ali, M. Asim, T.A. Khan, Low cost adsorbents for the removal of organic pollutants from wastewater, J. Environ. Manage., 113 (2012) 170–183.
[11] A.A. Azzaz, S. Jellali, H. Akrout, A.A. Assadi, L. Bousselmi, Optimization of a cationic dye removal by a chemically modified agriculture by-product using response surface methodology: biomasses characterization and adsorption properties, Environ. Sci. Pollut. Res., 24 (2017) 9831–9846.
[12] A.A. Azzaz, S. Jellali, A.A. Assadi, L. Bousselmi, Chemical treatment of orange tree sawdust for a cationic dye enhancement removal from aqueous solutions: kinetic, equilibrium and thermodynamic studies, Desal. Wat. Treat., 57 (2016) 22107–22119.
[13] S.L. Avelar, W.E.P. Martim, M.P. Vianna, A new occurence of *Limnoperna fortunei* (Dunker 1856) (Bivalvia, Mytilidae) in the state of Sao Paulo, Brazil, Braz. J. Biol., 64 (2003) 739–742.
[14] M.D. Oliveira, D.F. Calheiros, C.M. Jacobi, S.K. Hamilton, Abiotic factors controlling the establishment and abundance of the invasive golden mussel *Limnoperna fortunei*, Biol. Invasions, 13 (2011) 717–729.
[15] G. Darrigran, G. Pastorino, The Recent Introduction of Asiatic Bivalve, *Limnoperna fortunei* (Mytilidae) into South America, The Veliger, 38 (1995) 171–175.
[16] G.Y. Yao, M.Z. Xu, X.H. An, Concrete deterioration caused by freshwater mussel *Limnoperna fortunei* fouling, Int. Biodeterior. Biodegrad., 121 (2017) 55–65.
[17] L. Wachholz, R.V. Nunes, J. Broch, C. De Souza, Possibilidade do uso de Mexilhão Dourado contaminado com metais tóxicos em dietas para frangos de corte, Rev. Colomb. Ciência Anim., 9 (2017) 227–235.

[18] G. Darrigran, C. Damboronea, Bio-invasion del mejillon dorado en el continente americano, Anim. Genet., 39 (2006) 561–563.
[19] S. Peña-Rodríguez, D. Fernández-Calviño, J.C. Nóvoa-Muñoz, M. Arias-Estévez, A. Núñez-Delgado, M.J. Fernández-Sanjurjo, E. Álvarez-Rodríguez, Kinetics of Hg(II) adsorption and desorption in calcined mussel shells, J. Hazard. Mater., 180 (2010) 622–627.
[20] M. El Haddad, A. Regti, M.R. Laamari, R. Slimani, R. Mamouni, S. El Antri, S. Lazar, Calcined mussel shells as a new and eco-friendly biosorbent to remove textile dyes from aqueous solutions, J. Taiwan Inst. Chem. Eng., 45 (2014) 533–540.
[21] N. Seco-Reigosa, S. Peña-Rodríguez, J.C. Nóvoa-Muñoz, M. Arias-Estévez, M.J. Fernández-Sanjurjo, E. Álvarez-Rodríguez, A. Núñez-Delgado, Arsenic, chromium and mercury removal using mussel shell ash or a sludge/ashes waste mixture, Environ. Sci. Pollut. Res., 20 (2013) 2670–2678.
[22] Y.S. Ho, Citation review of Lagergren kinetic rate equation on adsorption reactions, Scientometrics, 59 (2004) 171–177.
[23] Y.S. Ho, G. McKay, Pseudo-second-order model for sorption processes, Process Biochem., 34 (1999) 451–465.
[24] N. Ayawei, A.N. Ebelegi, D. Wankasi, Modelling and interpretation of adsorption isotherms, J. Chem., 2017 (2017) 1–11.
[25] C. Rombaldi, J.L. De Oliveira Arias, G.I. Hertzog, S.S. Caldas, J.P. Vieira, E.G. Primel, New environmentally friendly MSPD solid support based on golden mussel shell: characterization and application for extraction of organic contaminants from mussel tissue, Anal. Bioanal. Chem., 407 (2015) 4805–4814.
[26] L.A. Araujo, C.O. Bezerra, L.F. Cusioli, M.F. Silva, L. Nishi, R.G. Gomes, R. Bergamasco, Moringa oleifera biomass residue for the removal of pharmaceuticals from water, J. Environ. Chem. Eng., 6 (2018) 7192–7199.
[27] Z. Nan, Z. Shi, B. Yan, R. Guo, W. Hou, A novel morphology of aragonite and an abnormal polymorph transformation from calcite to aragonite with PAM and CTAB as additives, J. Colloid Interface Sci., 317 (2008) 77–82.
[28] H. Tap Van, L. Huong Nguyen, V. Dang Nguyen, X. Hoan Nguyen, T. Hai Nguyen, T. Vinh Nguyen, S. Vigneswaran, J. Rinklebe, H. Nguyen Tran, P. District, H. Chi Minh City, Characteristics and mechanisms of cadmium adsorption onto biogenic aragonite shells-derived biosorbent: batch and column studies, J. Environ. Manage., 241 (2019) 535–548.
[29] J.H. Shariffuddin, M.I. Jones, D.A. Patterson, Greener photocatalysts: hydroxyapatite derived from waste mussel shells for the photocatalytic degradation of a model azo dye wastewater, Chem. Eng. Res. Des., 91 (2013) 1693–1704.
[30] L. Lonappan, T. Rouissi, R. Kumar, S.K. Brar, A. Avalos, M. Verma, R.Y. Surampalli, J.R. Valero, Adsorption of methylene blue on biochar microparticles derived from different waste materials, Waste Manage., 49 (2016) 537–544.
[31] Y.S. Ho, G. McKay, A comparison of chemisorption kinetic models applied to pollutant removal on various sorbents, Process Saf. Environ. Prot., 76 (1998) 332–340.
[32] S. Douven, C.A. Paez, C.J. Gommes, The range of validity of sorption kinetic models, J. Colloid Interface Sci., 448 (2015) 437–450.
[33] H.N. Tran, S.J. You, A. Hosseini-Bandegharaei, H.P. Chao, Mistakes and inconsistencies regarding adsorption of contaminants from aqueous solutions: a critical review, Water Res., 120 (2017) 88–116.
[34] K.C. Bedin, A.C. Martins, A.L. Cazetta, O. Pezoti, V.C. Almeida, KOH-activated carbon prepared from sucrose spherical carbon: adsorption equilibrium, kinetic and thermodynamic studies for Methylene Blue removal, Chem. Eng. J., 286 (2016) 476–484.
[35] S.W. Nam, D.J. Choi, S.K. Kim, N. Her, K.D. Zoh, Adsorption characteristics of selected hydrophilic and hydrophobic micropollutants in water using activated carbon, J. Hazard. Mater., 270 (2014) 144–152.
[36] K.J. Mellish, R.D. Cox, D.I. Vernon, J. Griffiths, S.B. Brown, In Vitro photodynamic activity of a series of Methylene Blue analogues, Photochem. Photobiol., 75 (2004) 392.